

Automated artifact-free seafloor surface reconstruction with two-step ODETLAP (Ph.D. Showcase)

Tsz-Yam Lau
Rensselaer Polytechnic Institute
110, Eighth Street
Troy, NY, USA
laut@cs.rpi.edu

W. Randolph Franklin
Rensselaer Polytechnic Institute
110, Eighth Street
Troy, NY, USA
mail@wrfranklin.org

ABSTRACT

We present an updated artifact-free seafloor surface reconstruction scheme which preserves more terrain features than our previous attempt using overdetermined Laplacian Partial Differential Equation (ODETLAP) and automates the adjustment of smoothing parameter. The high resolution version of such a surface fitting problem remains a challenge since we are still confined to extremely unevenly distributed depth samples collected along and near the ships, in which case numerous generic reconstruction algorithms generate unacceptable surfaces featuring abnormal depth fluctuations which are correlated with the trackline locations. Previously we reported the use of ODETLAP, which integrates data-density-dependent smoothing into the reconstruction process, to generate surfaces which are free from such acquisition footprint. However, this scheme still suffers from certain terrain feature loss due to smoothing, and the reliance of human to decide appropriate smoothing factor. This paper aims to fix these two problems with a two-step ODETLAP procedure. The procedure first applies an accuracy-biased ODETLAP to complete the missing depth data from the given samples. After that, the vigorous depth fluctuations along the tracklines are to be removed by applying a smoothing-biased ODETLAP on the completed grid. To decide the optimal smoothing factor automatically, the procedure computes the areas occupied by individual bumps on the reconstructed surface. A surface suffering heavily from the artifacts has many areas of small values but few with big values. Smoothing reduces such skewness. We find that for many datasets, the artifact is mostly gone when the coefficient of variation of the areas drops to around 1.5. Using that value to gauge the smoothing factor, the automated scheme successfully generates artifact-free seafloor surfaces within a limited error budget.

Categories and Subject Descriptors

I.3.5 [Computing Methodologies]: Computer Graphics
Computational Geometry and Object Modeling

Submitted for publication, July 2012. This research was partially supported by NSF grants CMMI-0835762 and IIS-1117277.

Keywords

GIS, ODETLAP, bathymetry, surface reconstruction, sparse height grid

1. INTRODUCTION

A bathymetric chart, the underwater equivalent of a topographic map, represents the depth and features of the ocean floor. This piece of data helps solve not only applications such as tsunami hazard assessment, communications cable and pipeline route planning, resource exploration, habitat management, and territorial claims under the Law of the Sea, but also fundamental Earth science questions, such as what controls seafloor shape and how seafloor shape influences global climate [12].

While wide-area, high-resolution ground heights can now be measured quickly with aerial electromagnetic survey technologies such as standard photogrammetry and LIDAR [10], the same is not true with seafloor depths. Good discussions on this issue are available at [12, 14]. In short, the problem is the 3000-5000 meters of salty water which masks the penetration of electromagnetic waves.

The altimeter method is an attempt for wide-area coverage. The method exploits the fact that the ocean surface has broad bumps and dips that mimic the topography of the ocean floor. By surveying the shape of the water surface instead, we avoid the need to shoot electromagnetic waves into the water, yet allowing us to deduce how the underlying seafloor looks like. However, it is reported that features on the ocean floor that are narrower than the average ocean depth of 3-5 kilometers do not produce measurable bumps on the ocean surface.

To obtain high-resolution data, we have no choice but to sail across the ocean, and on the way send out acoustic pulses to the seafloor. From the time it takes the pulses to leave the ship, be reflected by the seafloor and eventually get back the ship again, the ocean depths can be estimated. However, since ships travel slowly, the ocean remains largely uncharted. It has been estimated that 300 years are needed to cover the whole ocean area. With the most popular multibeam bathymetry technique[16], we can collect many data points with 10m resolution in a swath up to 10km wide along a ship's trackline. However, between the tracklines there is no data. In the southern oceans, these survey lines can sometimes be close together, but more often they are hundreds of kilometers apart [15]. Figure 1 demonstrates the spatial distribution of

such shipboard data samples in a few 10×10 degree regions.

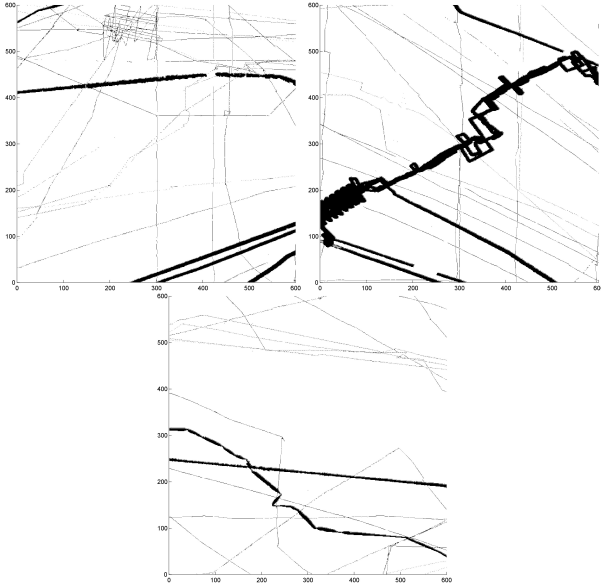


Figure 1: Locations with available depth samples. (Top left) Set 1: 30S-40S, 80E-90E. (Top right) Set 2: 40S-50S, 90E-100E. (Bottom) Set 3: 30S-40S, 90E-100E.

Since many analyses assume a full data grid, we have to do a *surface reconstruction*. The problem is defined over a spatial domain of dimensions $n \times n$. Available are the measured depth values of $k \ll n^2$ positions $(x_1, y_1), (x_2, y_2), \dots, (x_k, y_k)$, denoted as $h_{x_1, y_1}, h_{x_2, y_2}, \dots, h_{x_k, y_k}$. The task is to predict the depths for all the $n \times n$ positions in the domain, both those of the k known positions, and those of the remaining $n^2 - k$ unknown positions. This assumes for each possible location (i, j) within the domain, the corresponding predicted depth $z_{i, j}$ is single-valued; caves or overhangs are not allowed.

Acquisition footprint is the major problem suffered by seafloor surfaces reconstructed with general reconstruction schemes from those extremely unevenly distributed data, even with a few current bathymetry charts such as the one published by National Oceanic and Atmospheric Administration (NOAA) [9]. It refers to the artifact which is associated with the data-acquisition paths and hence makes the tracklines visible. The artifact is especially visible under *shaded relief*, a graphic technique which is often used to highlight the variations of a terrain surface [17]. Figure 2 shows how the reconstructed seafloor surfaces look like under a few such schemes such as inverse distance weighting (IDW) [13] and Kriging [4]. While both come up with a surface of a similar general shape, we observe abnormal depth fluctuations which are correlated with the trackline locations. Such correlated fluctuations do not make good sense. We aim at an artifact-free surface from which we cannot deduce the locations of the tracklines based on any clues on its surface. Meanwhile, the general shape as deduced from the given data should be preserved. One current solution, CleanTOPO2 [11], involves post-processing, manually removing the generated surfaces with Photoshop. As we are obtaining new trackline depth data from time to

time, it may become impractical to do the manual process every time the database expands. There arises a need for an automatic way to generate artifact-free reconstructed surfaces.

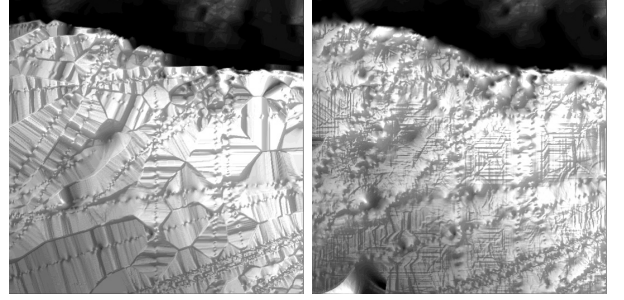


Figure 2: Set 1 reconstructions with (Left) Inverse Distance Weighting (IDW), (Right) Kriging.

Our previous work proposes the use of Overdetermined Laplacian Partial Differential Equation (ODETLAP) as a solution. Its original version is designed with smoothing considered right in the reconstruction process, and yields much better reconstruction accuracy than conventional algorithm. At that time, we further improve its accuracy by allowing the smoothing factor to vary from places to places according to their individual smoothing need. Section 2 will give information about those methods.

This paper aims to improve that ODETLAP implementation in two ways. First, we find that quite a few terrain features have been lost in our original variable-smoothing ODETLAP, when we compare the result with the surface reconstructed with a highly-accurate factor. We fix it by a two-step approach which reconstructs a preliminary surface with ODETLAP of a high-accuracy setting, and then applying a smoothing-biased ODETLAP over that preliminary surface. Second, our previously reported implementation still relies on human to set smoothing parameters. We automate the process based on the distribution of bump areas. Details will be given in Section 3, before we conclude the paper in Section 4.

2. ODETLAP

We previously presented Overdetermined Laplacian Partial Differential Equation (ODETLAP) as the solution to this artifact-free surface reconstruction problem [5]. It was earlier presented in the context of lossy terrain compression [2, 20, 21]. It predicts neighboring terrain heights better than other conventional prediction schemes, making it a better candidate for compression and reconstruction. It can work with contour lines (continuous or intermittently broken), infer mountain tops inside a ring of contours, and enforce continuity of slope across contours. All these are favorable features of natural-looking terrains.

Its formulation sets up an overdetermined system $\mathbf{Az} = \mathbf{b}$, as shown in Figure 3, to solve for the depths of the whole seafloor depth grid \mathbf{z} . The system includes an exact equation for each of the k known-depth positions. That equation sets the depth value of the respective position to its known value. The system also contains an averaging equation for all n^2 positions. That equation attempts to regularize the respective

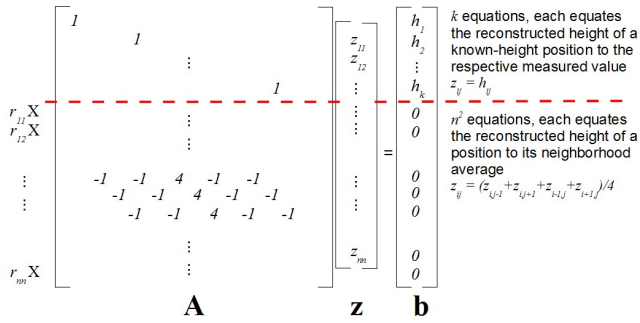


Figure 3: ODETLAP.

depth to the average of its immediate four neighbors. Through adjusting the weights $r_{i,j}$ of averaging equations, we can change how the errors are distributed over the equations and hence obtain terrain surfaces of the desired accuracy-smoothness tradeoff.

If the r values are low (e.g. 1), the system is *accuracy-centric*. The reconstructed values of the known-depth locations will be close to the measured values. However, acquisition footprint appears extensively as vigorous fluctuations along the tracklines, as shown in Figure 4, top left. Note that in areas with no data, the surface is relatively plain. This is superior to the surfaces done with conventional reconstruction schemes mentioned early, in which the artifact also affects those regions. To eliminate such artifacts, we can use the *smoothing-centric* version in which the if the r values are high (e.g. 50). Accuracy at known-depth locations (especially those with exceptional values) are sacrificed for a smooth surface as implied by the averaging equations, as shown in Figure 4, top right.

In its original version, we set all $r_{i,j}$ to be of the same value. To save unnecessary error budget, we propose adjusting the $r_{i,j}$ values for individual spatial locations in our previous paper. We observe that the trackline locations are usually of high data density and hence relatively higher smoothing. We ask the user to specify the smoothing factors for locations with lowest local sample density and locations with highest sample density, and then allow locations with intermediate data density to vary in between these two values. As a result, we achieve the surface of similar quality with a smaller error budget. Figure 4, bottom, shows a typical reconstruction results with such a variable-smoothing ODETLAP system.

The time complexity of ODETLAP is $O(n^3 + k)$. In practice, we transform the system to $\mathbf{A}^T \mathbf{A} \mathbf{z} = \mathbf{A}^T \mathbf{b}$ before solving for \mathbf{z} . In this equivalent system $\mathbf{A}' \mathbf{z} = \mathbf{b}'$ where $\mathbf{A}' = \mathbf{A}^T \mathbf{A}$ and $\mathbf{b}' = \mathbf{A}^T \mathbf{b}$, \mathbf{A}' is *symmetric positive definite*. We can then take advantage of the fast Cholesky factorization to keep the actual solving time to within seconds even for large datasets [7]. Also note that the matrix F is indeed a $n^2 \times n^2$ sparse matrix because the number of non-zero entries in each row is upper bounded by the number of possible immediate neighbors, which is 4. With the recent advances of graphical display units (GPU) in solving sparse linear systems [1, 6, 8], this approach has the potential to offer fast and efficient solutions to large data grids.

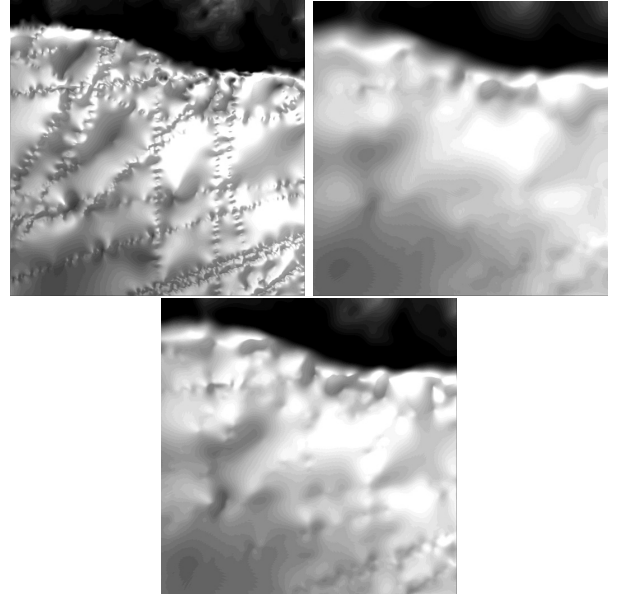


Figure 4: Set 1 reconstructions with ODETLAP: (Top left) accuracy-centric. (Top right) smoothing-centric. (Bottom) intermediate, with variable smoothness factors.

3. AUTOMATED TWO-STEP ODETLAP

Figure 5 gives the flow diagram of the automated two-step ODETLAP as the solution of the automated artifact-free seafloor surface reconstruction problem. Below we will describe the algorithm in terms of its two feature characteristics, namely *terrain feature preservation* and *automated smooth factor determination*.

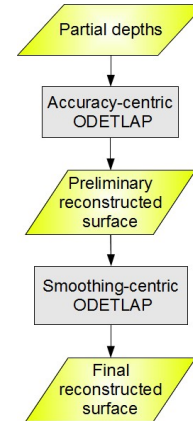


Figure 5: Two-step ODETLAP workflow.

3.1 Terrain feature preservation

Our new algorithm first reconstructs a highly-accurate preliminary surface from the available depth data, and then smoothes that preliminary surface.

In the first step which reconstructs a preliminary seafloor surface, we choose ODETLAP since this reconstruction scheme works best in deducing the missing seafloor depth data. Also, with this scheme the artifact is concentrated at the track-

lines only. This makes it easier to develop an algorithm that detects the severity of the problem and facilitate the automated determination of smoothing factors, as described in the following subsection. We set the weighting between the exact equations and the averaging equations to be 1:1. We find that beyond that point, increasing the weightings of the exact equations does not change the accuracy of the preliminary terrain too much as does the final terrain of the two-step ODETLAP procedure.

In the second step which smoothes the preliminary surface, we once again pick ODETLAP since this scheme provides better smoothing of the artifacts than others. Figure 6 shows the reconstructed terrain after being smoothed by a mean filter using an error budget comparable to that of ODETLAP smoothing. As you can see, while artifact is almost gone with ODETLAP smoothing, it is not the case with the mean filter. This illustrates the capability of our scheme in distributing the limited error budget to the smoothing of appropriate things.

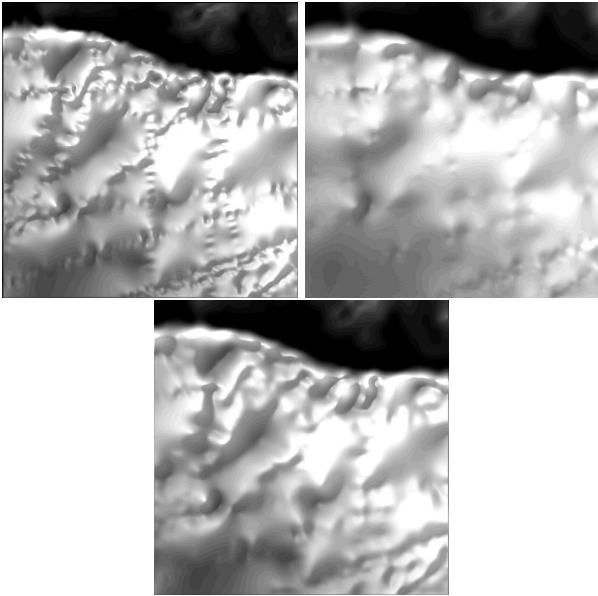


Figure 6: Set 1 reconstructed seafloor surfaces with mean error around 130m. (Top left) a mean filter with a square structure element of length 10, (Top right) variable-smoothness ODETLAP, (Bottom) two-step ODETLAP.

The only variable of this algorithm is essentially the smoothing factor in the second step. Figures 7–9, left, show how the surface varies as smoothing increases. A higher smoothing factor means a higher mean error but at the same time better smoothing-out of the small bumps along the tracklines. When compared with our original implementation which requires the specification of the lower and upper smoothing factors, we now have one fewer degree of freedom, make it easier to adjust. Also, terrain features (that is, relatively low-frequency depth variations) are preserved as long as the higher-frequency variations are still there. Both make our new scheme better than our previous schemes and other conventional algorithms. Figure 6 also presents the reconstructed surface using our previously presented variable-smoothing

ODETLAP mentioned in Section 2. In that surface, even though acquisition footprint is also almost gone, we also lose quite a few terrain features.

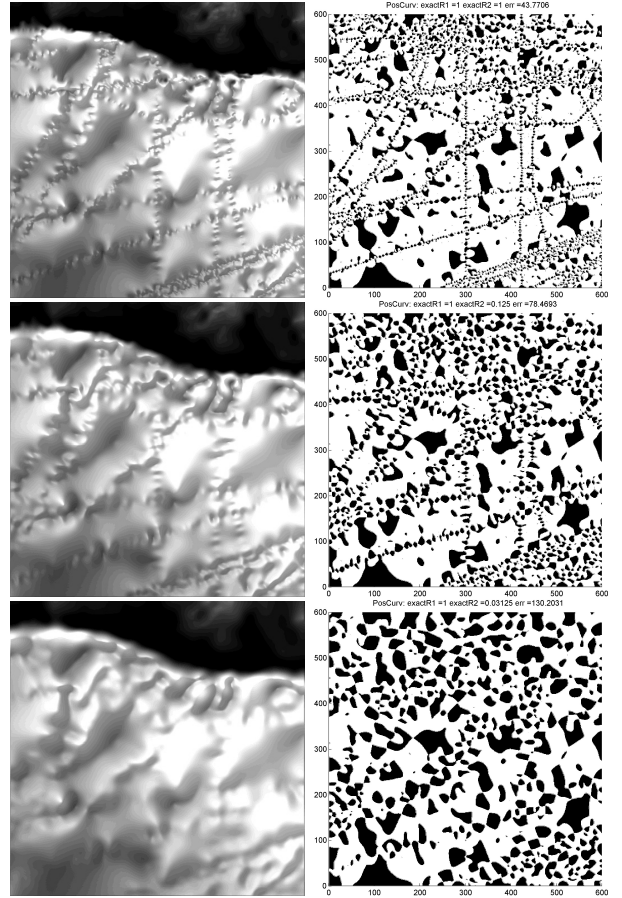


Figure 7: (Left) Set 1 reconstructed seafloor surfaces. (Right) Respective positive Gaussian curvature locations. The mean errors, from top to bottom, are around 44m, 78m and 130m respectively.

3.2 Automated smoothing determination

The above two-step procedure features a single parameter controlling the smoothing of the final reconstructed seafloor surface. To allow automated determination of the optimal smoothing level, first we need to convert the acquisition footprint of a surface to a form that is recognizable by computers. After several experiments, we find that the connected components in the graph of positive Gaussian curvature do a good job in indicating the locations of the shaded relief, as in some other research [3]. As shown on the right hand side of Figures 7–9, the artifact appears as relatively small patches concentrated at the trackline locations.

As observed from the figures, smoothing helps enlarge those patches enlarged or simply hide them. With a small smoothing factor, along the tracklines we have a huge number of small such patches. This is in contrast with regions with no data where there are few, much bigger patches. On increasing smoothing, the bumps along the tracklines become fewer and bigger, while those in no-data areas hardly change in

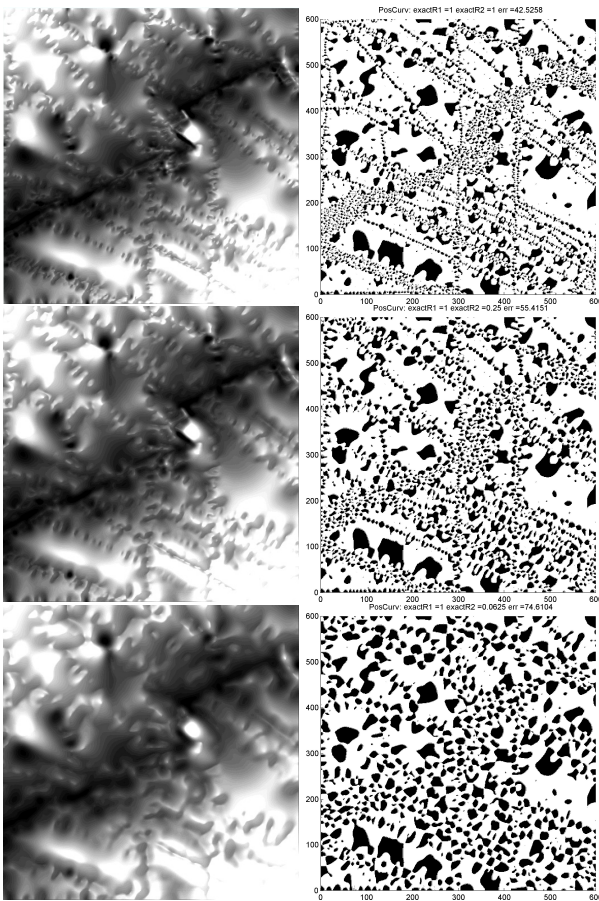


Figure 8: (Left) Set 2 reconstructed seafloor surfaces. (Right) Respective positive Gaussian curvature locations. The mean errors, from top to bottom, are around 43m, 55m and 75m respectively.

terms of both areas and quantity. This leads to a drop of the variations among the patch areas, as shown in Figure 10.

To utilize the above phenomenon for automated smoothing factor determination, we first apply a morphological erosion [19] with a 3-pixel-width square component on the positive Gaussian curvature graph to help discriminate the patches. We then compute the coefficient of variation, which is known as a normalized measure of dispersion of a probability distribution [18], of the patch areas. The acquisition footprint is found to have been almost gone when that coefficient drops to around 1.5. Figures 7–9, bottom, correspond to a smoothing level with around that value for the coefficient. Note that different datasets may need different error budgets to remove the artifacts. For example, while Set 3 requires a mean error budget as high as 214m to have the artifact removed, Set 2 needs 75m only. Using that coefficient to gauge smoothing helps reduce unnecessary smoothing and hence reduce the errors needed to achieve an artifact-free surface.

4. CONCLUSION

We have presented an improved ODETLAP procedure for the automated reconstruction of artifact-free seafloor surfaces within a limited error budget. It has the smoothing factor as

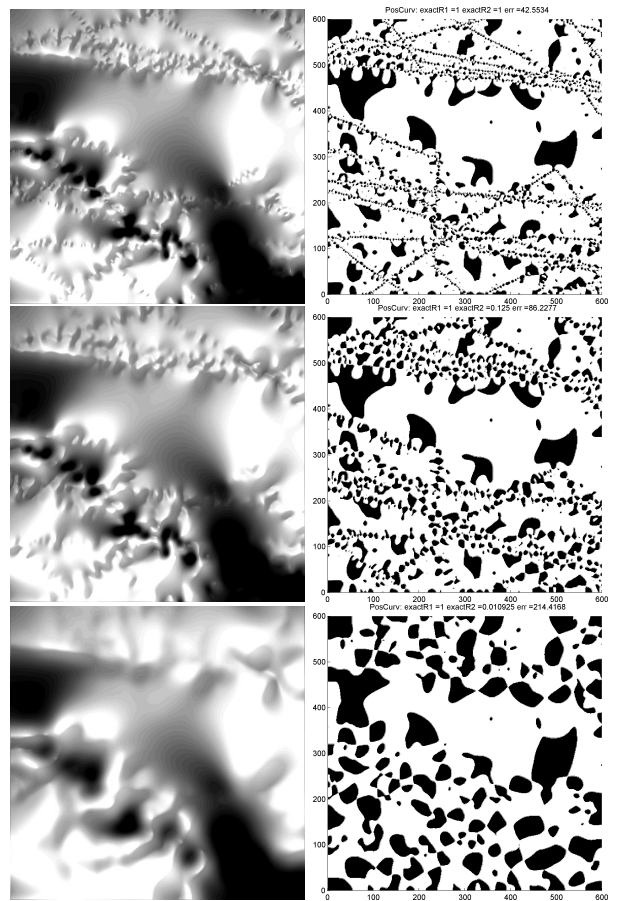


Figure 9: (Left) Set 3 reconstructed seafloor surfaces. (Right) Respective positive Gaussian curvature locations. The mean errors, from top to bottom, are around 43m, 86m and 214m respectively.

its only parameter, making it easier to adjust than our previous attempt that requires two parameter inputs. By smoothing an accurate reconstruction rather than a given measured values, we allow terrain features to be better preserved than the original scheme that reconstructs from the given measured values directly. To automate the adjustment of the smoothness parameter, we analyze the Gaussian curvature of the reconstructed surfaces. Areas of positive Gaussian curvatures highly resemble the locations of the bumps we observe on the shaded reconstructed surface. Increasing smoothing enlarges the small bumps and reduces their numbers along the tracklines and hence alleviates the acquisition footprint. When the coefficient of variation of such areas is around 1.5, the artifact is almost gone. We use this observation to determine the minimum smoothing needed to generate the artifact-free surface.

As for future work, we will look into the automatic stopping criterion further. More tests will be done on a variety of trackline depth samples. Even more accurate stopping criteria will be investigated. Our current work embraces data from the tracklines but not the altimeter measurements. It would be interesting to see how data from different sources could combine.

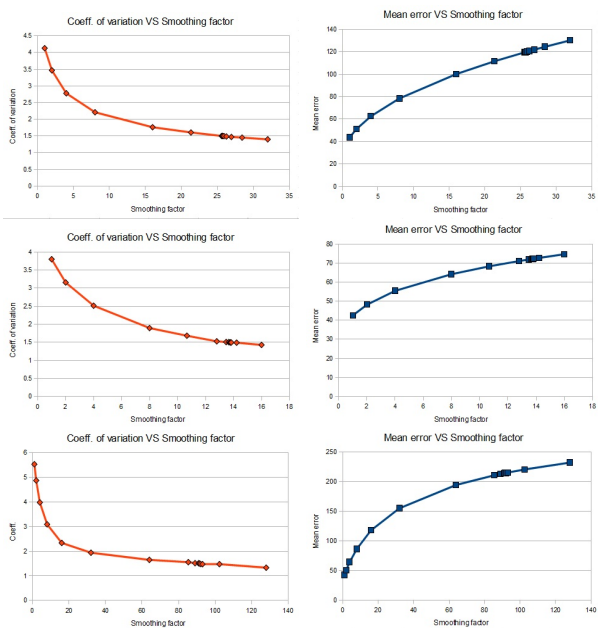


Figure 10: Coefficient of variation and mean error against smoothing factor. (Top) Set 1. (Middle) Set 2. (Bottom) Set 3.

5. REFERENCES

- [1] N. Bell and M. Garland. Implementing sparse matrix-vector multiplication on throughput-oriented processors. In *Proceedings of the Conference on High Performance Computing Networking, Storage and Analysis*, SC '09, pages 18:1–18:11, New York, NY, USA, 2009. ACM.
- [2] M. B. Gousie and W. R. Franklin. Augmenting grid-based contours to improve thin plate DEM generation. *Photogrammetric Engineering & Remote Sensing*, 71(1):69–79, 2005.
- [3] Y. Iwahori, S. Fukui, C. Fujitani, Y. Adachi, and R. J. Woodham. Relative magnitude of gaussian curvature from shading images using neural network. In *Proceedings of the 9th international conference on Knowledge-Based Intelligent Information and Engineering Systems - Volume Part I*, KES'05, pages 813–819, Berlin, Heidelberg, 2005. Springer-Verlag.
- [4] D. G. Krige. A statistical approach to some mine valuations and allied problems at the Witwatersrand. Master's thesis, University of Witwatersrand, 1951.
- [5] T.-Y. Lau, Y. Li, Z. Xie, and W. R. Franklin. Sea floor bathymetry trackline surface fitting without visible artifacts using ODETLAP. In *Proceedings of the 17th ACM SIGSPATIAL International Conference on Advances in Geographic Information Systems*, GIS '09, pages 508–511, New York, NY, USA, 2009. ACM.
- [6] Y. Li. *CUDA-accelerated HD-ODETLAP: a High Dimensional Geospatial Data Compression Framework*. PhD thesis, Rensselaer Polytechnic Institute, 2011.
- [7] Y. Li, T. Y. Lau, C. S. Stuetzle, P. Fox, and W. R. Franklin. 3D oceanographic data compression using 3D-ODETLAP. In *18th ACM SIGSPATIAL International Conference on Advances in Geographic Information Systems*, 2010.
- [8] D. Luebke, M. Harris, N. Govindaraju, A. Lefohn, M. Houston, J. Owens, M. Segal, M. Papakipos, and I. Buck. GPGPU: general-purpose computation on graphics hardware. In *Proceedings of the 2006 ACM/IEEE conference on Supercomputing*, SC '06, New York, NY, USA, 2006. ACM.
- [9] National Oceanic and Atmospheric Administration. Bathymetry data viewer. <http://maps.ngdc.noaa.gov/viewers/bathymetry/>, (retrieved Jul 2, 2012), 2012.
- [10] National Oceanic and Atmospheric Administration Coastal Services Center. LiDAR 101: An introduction to LiDAR technology, data, and applications. http://www.csc.noaa.gov/digitalcoast/data/coastallidar/_pdf/What_is_Lidar.pdf, (retrieved Feb 18, 2011), 2008.
- [11] T. Patterson. CleanTOPO2: Edited SRTM30 plus World Elevation Data. <http://www.shadedrelief.com/cleantopo2/>, (retrieved Jul 2, 2012), 2007.
- [12] D. T. Sandwell. Ocean Bumps and Dips. *The World & I*, 3:252–255, 1992.
- [13] D. Shepard. A two-dimensional interpolation function for irregularly-spaced data. In *Proceedings of the 1968 ACM National Conference*, pages 517–524, 1968.
- [14] W. H. Smith and D. T. Sandwell. Global sea floor topography from satellite altimetry and ship depth soundings. *Science Magazine*, 277, issue 5334, 1997.
- [15] W. H. Smith and D. T. Sandwell. Predicted seafloor topography: NGDC data announcement number: 94-MGG-04. <http://www.ngdc.noaa.gov/mgg/fliers/94mgg04.html>, (retrieved 6/8/2009), July 2008.
- [16] University of Rhode Island, Office of Marine Programs. Discovery of sound in the sea: Echo sounder-multibeam. <http://www.dosits.org/gallery/tech/osf/esm1.html>, (retrieved 6/8/2009), Mar. 2008.
- [17] Wikipedia. Cartographic relief depiction. http://en.wikipedia.org/wiki/Cartographic_relief_depiction, (retrieved Jul 2, 2012), 2012.
- [18] Wikipedia. Coefficient of variation. http://en.wikipedia.org/wiki/Coefficient_of_variation, (retrieved Jul 2, 2012), 2012.
- [19] Wikipedia. Erosion (morphology). http://en.wikipedia.org/wiki/Erosion_%28morphology%29, (retrieved Jul 2, 2012), 2012.
- [20] Z. Xie, M. A. Andrade, W. R. Franklin, B. Cutler, M. Inanc, D. M. Tracy, and J. Muckell. Approximating terrain with over-determined Laplacian PDEs. In *17th Fall Workshop on Computational Geometry*, IBM TJ Watson Research Center, Hawthorne NY, 2–3 Nov 2007. poster session, no formal proceedings.
- [21] Z. Xie, W. R. Franklin, B. Cutler, M. A. Andrade, M. Inanc, and D. M. Tracy. Surface compression using over-determined Laplacian approximation. In *Proceedings of SPIE Vol. 6697 Advanced Signal Processing Algorithms, Architectures, and Implementations XVII*, San Diego CA, 27 August 2007. International Society for Optical Engineering. paper 6697-15.